Published in final edited form as:
Neuroimage. 2008 July 15; 41(4): 1493–1503. doi:10.1016/j.neuroimage.2008.03.029.

Default-Mode Function and Task-Induced Deactivation Have Overlapping Brain Substrates in Children

Moriah E. Thomason[1], **Catherine E. Chang**[2], **Gary H. Glover**[3], **John D.E. Gabrieli**[4], **Michael D. Greicius**[5], and **Ian H. Gotlib**[1]

[1]Department of Psychology, Stanford University, Stanford, CA 94305

[2]Department of Electrical Engineering, Stanford University, Stanford, CA 94305

[3]Department of Radiology, Stanford University, Stanford, CA 94305

[4]Department of Brain and Cognitive Sciences, Massachusetts Institute of Technology, Cambridge, MA

[5]Department of Neurology, Stanford University School of Medicine, Stanford, California 94305

Abstract

The regions that comprise the functionally connected resting-state default-mode network (DMN) in adults appear to be the same as those that are characterized by task-induced decreases in blood-oxygen-level-dependent (BOLD) signal. Independent component analysis can be used to produce a picture of the DMN as an individual rests quietly in the scanner. Contrasts across conditions in which cognitive load is parametrically modulated can delineate neural structures that have decreases in activation in response to high-demand task conditions. Examination of the degree to which these networks subsume dissociable brain substrates, and of the degree to which they overlap, provides insight concerning their purpose, function, and the nature of their associations. Few studies have examined the DMN in children, and none have tested whether the neural regions that comprise the DMN during a resting condition are the same regions that show reduced activity when children engage in cognitive tasks. In this paper we describe regions that show both task-related decreases and spontaneous intrinsic activity at rest in children, and we examine the co-localization of these networks. We describe ways in which the DMN in 7-12-year-old children is both similar to and different from the DMN in adults; moreover, we document that task-induced deactivations and default-mode resting-state activity in children share common neural substrates. It appears, therefore, that even before adolescence a core aspect of task-induced deactivation involves reallocating processing resources that are active at rest. We describe how future studies assessing the development of these systems would benefit from examining these constructs as part of one continuous system.

Keywords

children; fMRI; default-mode; resting state; task-induced deactivation; functional connectivity

Correspondence should be addressed to: Moriah Thomason, Ph.D., Department of Psychology, Stanford University, Jordan Hall, Bldg. 420, Stanford, California 94305-2130, Tel: 650-725-0797, Fax: 650-725-5699, E-mail: moriah@stanford.edu.

Introduction

Over the past decade we have learned much about the function of the human brain while it is at 'rest', that is, unconstrained by task-related processes. The spatial reliability of the activation patterns observed at rest across both subjects and studies is arguably one of the more remarkable emergent features of resting state systems. Internally directed processes such as episodic memory, self-projection, and self-referential processing consistently activate regions of one resting state network that has earned the reputation as the brain's "default-mode" network (DMN) (Buckner and Carroll, 2007; Gusnard and Raichle, 2001; Wagner et al., 2005). Numerous functional imaging studies have provided evidence of task-induced decreases in brain activity relative to rest across the DMN (Binder et al., 1999; Gusnard and Raichle, 2001; Mazoyer et al., 2001; McKiernan et al., 2003; Shulman et al., 1997), suggesting that the resting state is dominated by internally directed thoughts. Moreover, investigators have shown that deactivation is adaptive: the extent to which individuals are able to 'turn down' response in the DMN during task engagement has been found to be related to successful performance (Daselaar et al., 2004; Otten and Rugg, 2001; Polli et al., 2005; Weissman et al., 2006).

In adults, the DMN has been found to include regions of the posterior cingulate cortex (PCC), precuneus, medial prefrontal cortex (MPFC), orbital frontal gyrus (OFG), anterior cingulate gyrus (ACC), inferolateral temporal cortex (ITC), parahippocampal gyrus (PHG), and lateral parietal cortex (LP) (Fox et al., 2005; Fransson, 2005; Greicius et al., 2003; McKiernan et al., 2003; Raichle et al., 2001; Shulman et al., 1997). Investigators using diverse methodologies with adults have identified this network in the brain's baseline state. Thus, to assess the DMN, researchers have examined: (i) the oxygen extraction fraction measured by positron-emission tomography (PET) at rest (Raichle et al., 2001); (ii) regions of greater PET blood flow or functional magnetic resonance imaging (fMRI) BOLD activity during passive than during active tasks (Shulman et al., 1997); and (iii) functional connectivity in brain regions implicated in the default-mode network during rest (Greicius et al., 2003).

Although this baseline state has been well documented in samples of adults, we know little about the DMN in children. Developmental fMRI studies have shown age effects in the magnitude of task-induced deactivations for the MPFC, subgenual anterior cingulate, and PCC, where greater deactivation is present in adults than in children (Marsh et al., 2006). In a recent resting-state functional connectivity study, Fair and colleagues (2007) identified more short-distance connections in children and more long-distance connections in adults. Importantly, one significant long-distance connection for which Fair et al. found strength to increase with age was between the PCC and the MPFC, components of the DMN. These studies provide evidence that the DMN may become more robust with age and that strengthening between nodes within the DMN is accompanied by weakening in the association of default-mode components with other networks. Clearly, it is important to understand these complementary processes in children and to evaluate these results in the context of the broad extant literatures for each domain in adults.

Examination of the DMN in children is important for two reasons. First, the low frequency BOLD fluctuations that characterize the resting state reflect intrinsic spontaneous neural activity in the absence of task constraints (Biswal et al., 1995; Fox et al., 2005; Greicius et al., 2003). Second, resting-state functional connectivity measures are postulated to reflect anatomical connectivity (Koch et al., 2002; Quigley et al., 2003). Understanding the ways in which children and adults differ in their intrinsic spontaneous neural activity is important because this activity is associated with stimulus-independent thought. Marsh and colleagues (2006) reasoned that greater deactivation as a function of increased age was likely to represent greater engagement of adults in self-monitoring and free associative thought processes during their easier baseline task. Critical questions remain about whether and how areas of greater

spontaneous activity across coherent networks at rest in children are similar to or different than published studies and meta-analyses conducted with adult participants.

The present study was designed to address questions related to nature of the DMN in children. We used fMRI to examine whether children demonstrate coherent spontaneous brain activity in the same default-mode regions that have been described in adults, and whether regions that are activated as part of the DMN are associated with regions that deactivate with increasing task demands. We administered spatial and verbal working memory (WM) tasks to children, varying the amount of information that they were required to maintain in WM so that we could delineate the neural substrates of decreased response in high-demand conditions. Including both verbal and spatial WM tasks allowed us to distinguish between domain-specific and superordinate task deactivations. Moreover, including multiple loads permitted us to examine parametric changes in activations as a function of the amount of information held in WM. We assessed the DMN during resting state in an independent age-matched cohort of children in order to examine the overlap in networks between task-induced decreases and task-independent spontaneous resting-state function. We summarized the peaks of our clusters in resting-state functional connectivity data and in task-induced deactivation data, and compared our findings to published peaks in these kinds of studies in adults.

Materials and Methods

Participants

Participants were recruited through fliers at Stanford University and in the surrounding community and through postings on Craigslist (a community based, free advertisement website), and were paid for their participation. Inclusion criteria included being ages 7-12, right-handed, having no past or current threshold psychopathology, being fluent in English, and having no moderate or severe learning disorder. Parents and their children gave informed consent and assent, respectively, as approved by the Stanford Institutional Review Board. Children participated in a behavioral assessment and orientation session prior to scan scheduling, and subsequently participated in either one or two fMRI scan sessions, depending on the study for which they were recruited. WM participants (N=14, mean age 9.9 years, range 7 to 11 years) were scanned in two sessions (one verbal WM session and one spatial WM session); resting-state participants (N=16, mean age 10.43 years, range 9 to 12 years) were scanned in one session.

Behavioral assessment

Participants in the WM study completed a behavioral assessment during their initial visit to the lab that included subtests from Woodcock-Johnson Tests of Cognitive Ability and the Wechsler Intelligence Scale for Children to derive WM performance scales (Digit Span and Block Span) and processing speed performance scales (Visual Matching, Symbol Search, and Digit Symbol-Coding). Children's scores on each subtest were converted to z-scores and averaged separately across the WM and processing speed performance scales to yield two composite z-scores for each participant. These behavioral measures permitted us to assess cognitive performance outside of the scanner and, as previous investigators have done, to examine associations between these measures and BOLD response (Klingberg et al., 2002).

During fMRI of WM, visual stimuli were presented using PsyScope (Macwhinney et al., 1997) on a Macintosh G4 computer and were back-projected onto a screen viewed through a mirror mounted above the participant's head. Participants indicated their responses with their right hand on a button-pad interfaced to the PsyScope button box. Spatial and verbal WM tasks were designed to be similar to each other. Pilot behavioral data were used to equate difficulty of the different loads for the spatial and verbal tasks. The task design was similar to that used

in previous fMRI WM studies (Jonides et al., 1993; Reuter-Lorenz et al., 2000; Smith et al., 1996). Thus, the spatial and verbal WM tasks used equivalent stimuli sequences, timing, and motor response characteristics; they differed only in the type of information held in mind and in the number of items maintained.

Each WM trial began with a central fixation cross, followed by presentation of successive encoding, maintenance, and retrieval phases (Thomason et al., in press). Participants were instructed to remember the information in the encoding display (either spatial locations defined by circles and rings or letters, shown for 1500 msec), to maintain the information over a delay period of either 100 msec (no maintenance) or 3000 msec (maintenance) during the presentation of a fixation cross, and then to indicate whether a test probe (either a spatial location or a letter) shown for 1500 msec matched the encoding display. For the spatial encoding displays, visual locations were indicated by 1, 3, or 5 target dots randomly arrayed across four invisible concentric circles centered around a fixation cross. At retrieval, participants saw a single outline circle encircling (or not encircling) the location of one of the dots from the encoding display. For the verbal encoding displays, there were 2, 4, or 6 upper-case letters arranged in a concentric circle around a fixation cross. At retrieval, participants saw a single lower-case letter that was (or was not) one of the letters from the encoding display. For both verbal and spatial trials, participants pressed one of two buttons to indicate either a match or a mismatch between probe and target items (location or letter).

Experimental and control blocks used equivalent stimulus sequences and motor response characteristics. Experimental blocks included the 3000 msec maintenance delay between encoding and retrieval, whereas control blocks did not require maintenance; they included only a brief perceptual delay of 100 msec. The number of items presented in the encoding and retrieval phases were matched for experimental and control blocks at each load, but a single (repeated) letter was presented in the verbal control trials and a single target location was presented in the spatial control trials and all trials were 5400 msec long. Thus, the control task matched the experimental task for perceptual and response factors, and duration. Four trials were presented in each block and the design did not require rest between blocks or cueing of participants to trial type. Thus, presentation across blocks was continuous. All scans consisted of 72 trials (36 experimental, 36 control, 50% match in each condition) in pseudo-random order alternating between experimental and control blocks. Each scan involved one kind of material with one load, and each lasted 6 minutes and 28 seconds.

During the resting-state experiment participants completed a six-minute scan during which they were instructed to lay still with eyes closed.

Behavioral analysis

Behavioral accuracy (% correct) and median reaction time (RT) data were analyzed using two-way (Material Type [spatial, verbal] × Load [low, medium, high]) repeated-measures analyses of variance (ANOVAs), correcting for non-sphericity.

Movement Analysis

For each participant the translational movement during scans was calculated in millimeters, and the rotational motion was calculated in radians based on the SPM2 parameters for motion correction of the functional images.

fMRI Acquisition Procedures

Magnetic resonance imaging was performed on a 3.0 T GE whole-body scanner. Participants were positioned in a purpose-built single channel T/R head coil and stabilized by padded clamps and a bite bar formed with dental impression wax (made of Impression Compound

Type I, Kerr Corporation, Romulus, MI) to reduce motion-related artifacts during scanning. For the WM study, 23 axial-oblique slices were taken with 4mm slice thickness, 1mm skip; for the resting-state study, 29 axial slices were taken with 4mm slice thickness. High-resolution T2-weighted fast spin echo structural images (TR = 3000ms, TE = 68ms, ETL=12) were acquired for anatomical reference. A T2*-sensitive gradient echo spiral in/out pulse sequence (Glover & Law, 2001) was used for all functional imaging (TR = 1500ms, TE = 30ms, flip angle = 70°, FOV = 24 cm, 64 × 64 for WM participants; TR = 2000ms, TE = 30ms, flip angle = 77°, FOV = 22 cm, 64 × 64 for resting state participants). An automated high-order shimming procedure, based on spiral acquisitions, was used to reduce B0 heterogeneity (Kim et al., 2002). Spiral in/out methods have been shown to increase signal-to-noise ratio and BOLD contrast-to-noise ratio in uniform brain regions, as well as to reduce signal loss in regions compromised by susceptibility-induced field gradients generated near air-tissue interfaces such as PFC (Glover and Law, 2001). Compared to traditional spiral imaging techniques, spiral in/out methods result in less signal dropout and greater task-related activation in PFC and medial temporal regions (Preston et al., 2004). A high-resolution volume scan (WM participants: 124 slices, 1.2mm slice thickness; resting-state participants: 144 slices, 1mm slice thickness) was collected for every participant using a spoiled grass gradient recalled (SPGR) sequence for T1 contrast (WM participants: TR = 8.9ms, TE = 1.8ms, TI = 300ms, flip angle = 15°, FOV = 24 cm, 256 × 192; resting-state participants: TR = 3000ms, TE = 68ms, TI = 500ms, flip angle = 11°, FOV = 25 cm, 256 × 256).

fMRI Analysis

fMRI data were preprocessed using SPM (Wellcome Dept of Cognitive Neurology, http://www.fil.ion.ucl.ac.uk/spm). Preprocessing included image realignment and co-registration of functional and anatomical images. Functional images were normalized to the Montreal Neurological Institute (MNI) template, using the participant-specific transformation parameters created by fitting grey matter segmented anatomical images to the single reference standard SPM grey matter template. Following normalization, all participant images were visually inspected, and it was determined that for five of the resting-state image sets the normalization was suboptimal. For these five participants an alternative mean functional image fit to the standard SPM EPI template was used to derive normalization parameters. Images were smoothed with a 6mm Gaussian kernel to decrease spatial noise.

Further WM processing for each participant was performed using SPM2. Contrast images created for each WM participant at each load level (experimental task > control task) were analyzed in a random-effects analysis to determine areas of task-induced deactivation across spatial and verbal WM scans. Further resting-state processing for each participant was performed using FSL (http://www.fmrib.ox.ac.uk/fsl/) and custom MATLAB routines. Preprocessed functional images were concatenated across the run using FSL avwmerge. The resulting single four-dimensional functional image was then analyzed using FSL melodic Independent Component Analysis (ICA) software. Using an automated MATLAB analysis routine developed for previous studies (Greicius et al., 2007; Greicius and Menon, 2004; Greicius et al., 2004), we selected the ICA component that best matched the default-mode brain network. Any component in which high-frequency signal (> 0.1 Hz) constituted more than 50% of the Fourier spectrum power was removed from consideration.

Participants' best-fit ICA component images were processed in a random effects analysis using SPM2. Best-fit images that result from the ICA analysis have z-scores assigned to each voxel. One-sample t-tests were used to compare the z-scores at each voxel to zero (the null hypothesis) within each participant group. Significant clusters were determined using height and extent thresholds of $p < 0.001$ and $k > 25$, respectively.

Region-of-interest (ROI) analyses were conducted for two different sets of ROIs. The first set included functionally defined regions for which we obtained a significant main effect of decreasing load for both spatial and verbal WM. The second set was based on previously published reports of task-induced decreases in activation in adults, described below. Functionally defined ROIs were used to determine whether there was an association between executive processing measures administered outside of the scanner and observed reduction in BOLD response. These analyses were conducted to examine the functional significance of task-induced decreases in activation. We examined 4mm spherical regions surrounding peak voxels in deactivations summarized in Table 2, for a total of 13 functionally-defined ROIs. In the second set of literature-based ROIs, we tested whether significant task-induced decreases that have been reported in adults also characterize young children. We tested only previously published coordinates that were located a maximum of 25mm from peaks in our data in order to reduce the search field while maximizing the possibility of obtaining significant change. We constructed 27 10mm spherical ROIs surrounding peak voxels reported by (Binder et al., 1999;Mazoyer et al., 2001;McKiernan et al., 2003;Shulman et al., 1997). Because task-induced deactivation reliably modulates a bilateral network across tasks and imaging modalities, we relaxed our selection of overlapping peak foci to include peaks occurring in homologous regions on the other side of the brain. For foci that occurred in the contralateral hemisphere in previous reports, we reversed the sign of the X coordinate if the resulting Euclidian distance between our observed peaks and the previously published peak would be less than 25mm. The anatomical regions/Brodmann's areas were computed by using in-house software that: (1) converts the MNI coordinates from SPM's set level statistics to Talairach coordinates via Matthew Brett's mni2tal conversion (discussed at: http://imaging.mrc-cbu.cam.ac.uk/imaging/MniTalairach); and (2) queries the Talairach database for anatomical locations/Brodmann's areas.

For all ROIs (13 functional ROIs and 27 literature-based ROIs; all peaks listed in Table 2), we extracted mean parameter estimates from each participant's contrast image (maintenance > no-maintenance) at each load level. The difference score (Δ) between low and high load was taken as a measure of BOLD decrease for each ROI. Correlations were computed between extracted Δ values for 13 functional ROIs and performance measures obtained outside of the scanner, and one-sample t-tests were conducted to compare extracted Δ values for the 27 literature-based ROIs to zero.

Finally, we conducted Monte-Carlo simulations to determine whether the overlap between regions of task-induced decreases and the functionally connected DMN was significantly greater than would be expected by chance. Images of the DMN ($p<0.001$) and the conjunction map between verbal WM and spatial WM load decreases ($p<0.05$) were binarized, and isolated clusters (17 total) were extracted from the DMN image. On each iteration of the simulation, we conceptually formed a new image in which the DMN clusters were moved to random locations within the brain, independent of (but constrained to not overlap with) one another. The overlap between this randomized DMN map and the WM conjunction map was defined as the sum, over all DMN clusters, of the percentage of overlapping voxels within each cluster. In summing the fraction of overlap in each cluster, we were effectively normalizing by cluster volume, thereby allowing equal contribution from clusters of different sizes. A histogram of overlap values (null distribution) was generated from 5000 iterations, and significance was determined as the fraction of the histogram's area lying to the right of the actual (non-permuted) overlap value between the WM conjunction map and the DMN.

Results

Behavioral Data

As predicted, the main effect of load was significant for both experimental trial accuracy, $F(2,52) = 36.63$, $p < 0.01$, and reaction time (RT), $F(2,52) = 25.06$, $p < 0.001$; for both measures, performance declined with increasing load. The main effect of material type was not significant for accuracy, $F(1,26) = 1.14$, $p = 0.3$, or median RT, $F(1,26) = 0.03$, $p = 0.87$, indicating that participants did not perform differently on the spatial and verbal WM tasks. Behavioral results are summarized in Table 1. Given these results, and to improve the generality of our deactivation results, we combined data across the verbal and spatial WM tasks to examine regions that show decreasing BOLD activation with increasing WM load.

Movement

Average movement across spatial and verbal WM scans, (averaged across X, Y, and Z translational dimensions) $\bar{x} = 0.30$ mm and $\bar{x} = 0.26$ mm, respectively, was not significantly different, $t(26) = 0.55$, $p = 0.59$. Average movement during resting state ($\bar{x} = 0.14$ mm) was significantly lower than was the case for during both spatial, $t(28) = 2.59$, $p < 0.05$, and verbal WM tasks, $t(28) = 2.87$, $p < 0.01$. Rotational movement (average for pitch, roll, and yaw) did not differ significantly among these comparisons. Although there was only modest translational movement in the WM scans (< 0.3 mm), we covaried movement in subsequent analyses to examine its potential effect. There were not significant differences in activation maps with and without covarying movement.

fMRI of WM task-induced deactivations

Consistent with reports in adults, children exhibited decreases in activation with increased WM load in limbic regions, PCC extending into the precuneus, middle frontal gyrus, sensorimotor cortices, and parietal regions (Fig. 1). We compared peak decreases in children to areas that have shown maximal deactivations in four widely cited studies of adults (Binder et al., 1999;Mazoyer et al., 2001;McKiernan et al., 2003;Shulman et al., 1997). In particular, we compared the primary foci in the present data to data reported in adults across different tasks, stimuli, and imaging modalities to examine whether our findings with children were similar to those obtained with adults. Regions of significant task-induced deactivation are summarized in Table 2, along with Euclidian distances between observed foci in studies of adults and peaks in the present data set. Activation decreases in children were quantified for ROIs of 10mm diameter constructed around peaks reported in the surveyed adult imaging data. The resulting Δ values are included in Table 2. Several ROIs demonstrated significance or a trend for significance when Δ values in these regions were analyzed, replicating with children in the present study significant changes in these regions previously found in adults. Even though some of the deactivations in these ROIs did not reach significance, all of these ROIs demonstrated deactivation with increased cognitive load.

Although there were a number of similarities between results reported in studies of deactivation in adults and the present findings with children, it is also important to highlight three specific differences. First, two of the peak foci found in our child data were left-right flipped from foci reported in adults. Second, three peak coordinates obtained in our data were not localized near peak foci in previously published findings with adults (shaded in grey in Table 2). Finally, for six peak foci reported in two or more of the four studies conducted with adults, we did not obtain significant decreases in the present study; these are listed in Table 3.

Cognitive measures taken outside of scanner (Table 4) were significantly correlated with the decrease in BOLD signal, or Δ, between low and high loads for 2 of the 13 functional deactivation foci. Composite z-scores averaged across WM tasks (Block Span and Digit Span)

were significantly correlated with BOLD decreases across load in the left postcentral gyrus (BA 3; -36,-27, 49), r = .608, $p < 0.05$. Composite z-scores averaged across speed of processing tasks (Digit Symbol, Visual Matching and Cross Out) were significantly correlated with BOLD decreases across load in the right middle frontal gyrus (MFG) (BA 8/9; 32, 23, 36), r = .558, $p < 0.05$. Values of Δ and behavioral z-scores are plotted in Fig. 2. These peaks correspond to ROIs 12 and 13 in Table 2 and Figure 1.

fMRI of default-mode functional connectivity in development

The primary regions of the DMN identified in the present sample of children are the same as those that have been consistently identified as part of the DMN in adults. Specifically, the four largest clusters of significant voxels were centered in the PCC/precuneus (BA 31/23), MPFC (BA 32/10), and bilaterally in the LP (BA 39), the same regions that are cited most reliably in adults (Fox et al., 2005; Fransson, 2005; Greicius et al., 2003). The spatial extent of the default-mode network is presented in Fig. 3, and peaks across the network are summarized in Table 5. To compare functional connectivity results obtained in the current study to those reported in previous investigations, we plotted peak foci from three functional connectivity rest studies in adults (Fox et al., 2005; Fransson, 2005; Greicius et al., 2003) along with the peaks obtained in our sample of children (see Fig 4) in a manner similar to that used by McKiernan et. al. in their 2003 meta-analysis. There were no regions identified as part of the DMN in two or more of the studies reviewed in Figure 4 that were not also identified as significant peaks in the present study.

It has been demonstrated that the ROI-based methods used in past studies yield the same results as the ICA-based method used in the current study (Greicius et al., 2004). To examine whether these approaches were also comparable in this study of children, we computed correlation maps by extracting BOLD timecourse from the peak PCC region, and then computing the correlation coefficients between that timecourse and the timecourses from all other brain voxels. The same regions of the DMN were identified by this alternate analysis: the PCC complex, bilateral lateral parietal, medial PFC, bilateral middle frontal regions (BA 8/9/46), parahippocampal gyrus, regions of the cerebellum, and a left middle temporal region (BA 21). Moreover, the consistency in the results of our ICA-based data and data from previous studies that used ROI-based methods provides further support for the comparability of these approaches.

Overlap of WM deactivations and resting state default network in children

An examination of the overlap of the networks implicated in task-related decreases in activation and resting-state DMN connectivity indicated that both approaches reliably extract the DMN. To quantify the degree of overlap obtained using these complementary approaches in the two samples, we conducted Monte-Carlo simulations, which revealed that the spatial overlap between the WM deactivation map and the default-mode network was significant ($p<0.05$). Fig. 5 presents the degree to which task-induced deactivations overlap with ICA-based resting functional connectivity in the DMN in children.

Discussion

The present study was designed to examine task-induced decreases in BOLD signal, the resting state DMN, and the relation between these in children. First, we demonstrated that, like adults, 7-11-year-old children show reliable reductions in BOLD response in the brain's DMN in response to increasing task demands or task difficulty. Second, in an independent 9-12-year-old cohort, we found resting-state functional connectivity across the DMN. Third, we quantified the degree of overlap between the DMN maps obtained by these complementary methods.

Important similarities and differences were obtained with respect to the relation between our developmental data and the previous literature to which it was compared. Considered collectively, the present data support the existence of an organized mode of brain function in children ages 7-12 that is present as a baseline or default state and is attenuated parametrically during goal-directed tasks. The data reported here demonstrate the co-localization of networks derived from task-induced decreases and from resting functional connectivity, suggesting that these processes fall along a single continuum. Like adults, 9-12-year-old children showed the largest DMN volume in the precuneus and PCC, regions that have been implicated in retrieval of self-related episodic memory (Cavanna and Trimble, 2006). The second- and third-largest volumes obtained in children's default-mode network included regions of the LP cortex: Brodmann's areas (BAs) 39, 40, 22, and 19, that are associated with conscious awareness and with semantic and conceptual processing (Binder et al., 1999). In addition, we found that children were characterized by several functionally connected clusters across regions of the ventromedial and dorsomedial prefrontal cortices, including MPFC regions associated with emotion processing (Bechara et al., 2000; Cunningham et al., 2004), and dorsomedial regions posited to mediate self-referential thought processes and mental-state reflection (Gallagher and Frith, 2003; Johnson et al., 2002). These observations mirror the nature of the DMN in studies of adults.

There were also differences between what has been reliably characterized in adults and what we found in our samples of children. Children showed significant task-related deactivations in three areas that have not been found consistently in adults: the postcentral-gyrus (BA3), a brain region that receives sensory feedback from the body; the insula (BA 13), a region that is postulated to integrate information relating to bodily states; and an inferior occipital region (BA18) that is important for visual processing. These differences may reflect greater integration between the DMN and sensory processing regions in children than in adults. On the other hand, although we collapsed across spatial and verbal WM domains to increase the generality of deactivation peaks, regions that are critical for cross-modal processing specific to both types of tasks would show significant deactivations. Thus, conclusions that these regions are unique to children should be tempered with a need for future studies to replicate these findings using different tasks and designs.

Previous studies support the conclusion that children of this age are not characterized by mature intrinsic connectivity networks. Marsh and colleagues showed that deactivations in the MPFC, anterior cingulate, and posterior cingulate scale with age (Marsh et al., 2006). In their study of resting state connectivity in children, Fair and colleagues found reduced dissociation between frontoparietal and cingulopercular control networks (Fair et al., 2007). Here, too, we observed in children reduced dissociation between brain networks, albeit between the DMN and elements of sensory networks. Fair and colleagues also observed that connection strength increased with age between the PCC and the MPFC, components of the DMN. This suggests that strengthening between nodes within the DMN is accompanied by weakening in the association of default-mode components with outside networks.

Our results with children also differed from previously published data with adults in that six regions that have been demonstrated to be a reliable part of the task-induced deactivation or DMN in adults were not significantly deactivated in our sample of children. To identify these regions, we calculated the Euclidian distance between every peak coordinate reported in four studies of task-induced deactivations in adults (Binder et al., 1999; Mazoyer et al., 2001; McKiernan et al., 2003; Shulman et al., 1997) that were not near to regions of significance in the current study. From these calculations we extracted peaks that were closely localized (within 30mm) across two or more of the adult studies. This resulted in the demarcation of adult deactivation peaks in prefrontal cortex (PFC) regions, parietal regions, somatosensory cortex, and ACC, not observed in our sample of children. Notably, most of the differences we

observed occurred in regions of the PFC (BA 10, 11,45, 46, 47). It is well established that the PFC plays an important role in response inhibition, emotion regulation and executive memory (Fuster, 2001; Miller and Cohen, 2001). Furthermore, the PFC is one of the last cortical regions to reach full structural maturation (Sowell et al., 1999; Yakovlev and Lecours, 1967) and it has been suggested that immaturity in cognitive control may be associated with an inability to recruit PFC regions (Bunge et al., 2002). It is of particular interest, therefore, that several regions that are reliably associated with task-induced decreases in adults were not replicated in our analysis of task-induced decreases in children.

There are aspects of functional imaging analysis that can complicate interpretation of results. In the present study we included any peak with a Euclidian distance < 25mm as similar and > 25mm as different. If we had decided to use a more restricted threshold, the similarities among groups would be reduced. Although regions 25mm away likely do not represent the same region (Hunton et al., 1996), clusters are likely to extend into overlapping anatomical regions. Similar criteria have been applied in past imaging studies of task-induced deactivation (Binder et al., 1999; Mazoyer et al., 2001). An additional caveat common to developmental fMRI studies is that investigators often collapse across a range of ages in which there are dynamic changes. It is well documented that there are rapid developmental gains between 7 and 12 years (Giedd et al., 1999; Giedd et al., 2006; Huttenlocher, 1979, 1990; Klingberg et al., 1999; Pfefferbaum et al., 1994; Yakovlev and Lecours, 1967). Consequently, collapsing across these ages in two samples with similar means but different ranges eliminates sensitivity to changes across these ages and could induce unequal variance in the groups included in the present study.

It will be important in future research to examine whether and how the differences we observed in the DMN in children are advantageous to cognitive processing. It may be that recruiting sensory network areas as part of the DMN is a form of compensation. Alternatively, it may be that the less children rely on sensory regions as part of this network, the better their performance on cognitive tasks. In the present study we identified two regions in the task-induced deactivation network in children in which the amount of deactivation (Δ value) was positively correlated with behavioral performance assessed out of the scanner. Of these regions, the postcentral gyrus was also characterized as being unique to children's default-mode network. Certainly, it is important that the significant correlations between Δ and the performance measures (WM capacity and processing speed) be interpreted with caution given the number of comparisons we computed. Furthermore, it is possible that the somatosensory deactivation is driven by the fact that there were fewer responses in the high WM-load condition. Nevertheless, the present data support the hypothesis that, for children, less deactivation in these specific sensory systems is associated with better behavioral performance.

The present study is the first to examine the relation between resting state network and task-induced deactivation in school-aged children. The nature of the task design (parametric modulation of WM load across both spatial and verbal domains) enabled us to identify a superordinate DMN in this age group and to compare results in our sample to published reports in adults. Examining a separate age-matched cohort, we used resting state functional connectivity to extract the DMN, hypothesizing that this method would yield a similar DMN in children, given that both methods have been shown reliably to identify this network in studies of adults. The results of this study indicate that children exhibit a DMN similar to adults, but that the system does still undergo important changes between middle childhood and adulthood.

Acknowledgments

The authors thank Christian E. Waugh for his helpful comments on an earlier draft of this paper, Meggy W. Wang, Hannah S. Kang, and Melissa L. Henry for their assistance in acquiring the fMRI scan data, and Daniel J. Yoo and Jesse Rissman for their assistance with data analysis. These studies were supported by grants MH074849 to IHG, MH071996 to MET, MH61426 to JDEG, and RR09784 to GHG.

References

Bechara A, Damasio H, Damasio AR. Emotion, decision making and the orbitofrontal cortex. Cereb Cortex 2000;10:295–307. [PubMed: 10731224]

Binder JR, Frost JA, Hammeke TA, Bellgowan PS, Rao SM, Cox RW. Conceptual processing during the conscious resting state. A functional MRI study. J Cogn Neurosci 1999;11:80–95. [PubMed: 9950716]

Biswal B, Yetkin FZ, Haughton VM, Hyde JS. Functional connectivity in the motor cortex of resting human brain using echo-planar MRI. Magn Reson Med 1995;34:537–541. [PubMed: 8524021]

Buckner RL, Carroll DC. Self-projection and the brain. Trends Cogn Sci 2007;11:49–57. [PubMed: 17188554]

Bunge S, Dudukovic N, Thomason M, Vaidya C, Gabrieli J. Immature Frontal Lobe Contributions to Cognitive Control in Children: Evidence from fMRI. Neuron 2002;33:301–311. [PubMed: 11804576]

Cavanna AE, Trimble MR. The precuneus: a review of its functional anatomy and behavioural correlates. Brain 2006;129:564–583. [PubMed: 16399806]

Cunningham WA, Raye CL, Johnson MK. Implicit and explicit evaluation: FMRI correlates of valence, emotional intensity, and control in the processing of attitudes. J Cogn Neurosci 2004;16:1717–1729. [PubMed: 15701224]

Daselaar SM, Prince SE, Cabeza R. When less means more: deactivations during encoding that predict subsequent memory. Neuroimage 2004;23:921–927. [PubMed: 15528092]

Fair DA, Dosenbach NU, Church JA, Cohen AL, Brahmbhatt S, Miezin FM, Barch DM, Raichle ME, Petersen SE, Schlaggar BL. Development of distinct control networks through segregation and integration. Proc Natl Acad Sci U S A 2007;104:13507–13512. [PubMed: 17679691]

Fox MD, Snyder AZ, Vincent JL, Corbetta M, Van Essen DC, Raichle ME. The human brain is intrinsically organized into dynamic, anticorrelated functional networks. Proc Natl Acad Sci U S A 2005;102:9673–9678. [PubMed: 15976020]

Fransson P. Spontaneous low-frequency BOLD signal fluctuations: an fMRI investigation of the resting-state default mode of brain function hypothesis. Hum Brain Mapp 2005;26:15–29. [PubMed: 15852468]

Fuster JM. The prefrontal cortex--an update: time is of the essence. Neuron 2001;30:319–333. [PubMed: 11394996]

Gallagher HL, Frith CD. Functional imaging of ‘theory of mind’. Trends Cogn Sci 2003;7:77–83. [PubMed: 12584026]

Giedd JN, Blumenthal J, Jeffries NO, Castellanos FX, Liu H, Zijdenbos A, Paus T, Evans AC, Rapoport JL. Brain development during childhood and adolescence: a longitudinal MRI study. Nat Neurosci 1999;2:861–863. [PubMed: 10491603]

Giedd JN, Clasen LS, Lenroot R, Greenstein D, Wallace GL, Ordaz S, Molloy EA, Blumenthal JD, Tossell JW, Stayer C, Samango-Sprouse CA, Shen DG, Davatzikos C, Merke D, Chrousos GP. Puberty-related influences on brain development. Molecular and Cellular Endocrinology 2006;254:154–162. [PubMed: 16765510]

Glover G, Law C. Spiral-in/out BOLD fMRI for increased SNR and reduced suceptibility artifacts. Magn Reson Med 2001;46:515–522. [PubMed: 11550244]

Greicius MD, Flores BH, Menon V, Glover GH, Solvason HB, Kenna H, Reiss AL, Schatzberg AF. Resting-State Functional Connectivity in Major Depression: Abnormally Increased Contributions from Subgenual Cingulate Cortex and Thalamus. Biol Psychiatry. 2007

Greicius MD, Krasnow B, Reiss AL, Menon V. Functional connectivity in the resting brain: a network analysis of the default mode hypothesis. Proc Natl Acad Sci U S A 2003;100:253–258. [PubMed: 12506194]

Greicius MD, Menon V. Default-mode activity during a passive sensory task: uncoupled from deactivation but impacting activation. J Cogn Neurosci 2004;16:1484–1492. [PubMed: 15601513]

Greicius MD, Srivastava G, Reiss AL, Menon V. Default-mode network activity distinguishes Alzheimer’s disease from healthy aging: evidence from functional MRI. Proc Natl Acad Sci U S A 2004;101:4637–4642. [PubMed: 15070770]

Gusnard DA, Raichle ME. Searching for a baseline: functional imaging and the resting human brain. Nat Rev Neurosci 2001;2:685–694. [PubMed: 11584306]

Hunton DL, Miezin FM, Buckner RL, vanMier HI, Raichle ME, Petersen SE. An assessment of functional-anatomical variability in neuroimaging studies. Human Brain Mapping 1996;4:122–139.

Huttenlocher P. Synaptic Density in Human Frontal-Cortex - Developmental Changes and Effects of Aging. Brain Research 1979;163:195–205. [PubMed: 427544]

Huttenlocher P. Morphometric study of human cerebral cortex development. Neuropsychologia 1990;28:517–527. [PubMed: 2203993]

Johnson SC, Baxter LC, Wilder LS, Pipe JG, Heiserman JE, Prigatano GP. Neural correlates of self-reflection. Brain 2002;125:1808–1814. [PubMed: 12135971]

Jonides J, Smith EE, Koeppe RA, Awh E, Minoshima S, Mintun MA. Spatial working memory in humans as revealed by PET. Nature 1993;363:623–625. [PubMed: 8510752]

Klingberg T, Forssberg H, Westerberg H. Increased brain activity in frontal and parietal cortex underlies the development of visuospatial working memory capacity during childhood. J Cogn Neurosci 2002;14:1–10. [PubMed: 11798382]

Klingberg T, Vaidya C, Gabrieli J, Moseley M, Hedehus M. Myelination and organization of the frontal white matter in children: a diffusion tensor MRI study. Neuroreport 1999;10:2817–2821. [PubMed: 10511446]

Koch MA, Norris DG, Hund-Georgiadis M. An investigation of functional and anatomical connectivity using magnetic resonance imaging. Neuroimage 2002;16:241–250. [PubMed: 11969331]

Macwhinney B, Cohen J, Provost J. The PsyScope experiment-building system. Spat Vis 1997;11:99–101. [PubMed: 9304758]

Marsh R, Zhu H, Schultz RT, Quackenbush G, Royal J, Skudlarski P, Peterson BS. A developmental fMRI study of self-regulatory control. Human Brain Mapping 2006;27:848–863. [PubMed: 16421886]

Mazoyer B, Zago L, Mellet E, Bricogne S, Etard O, Houde O, Crivello F, Joliot M, Petit L, Tzourio-Mazoyer N. Cortical networks for working memory and executive functions sustain the conscious resting state in man. Brain Res Bull 2001;54:287–298. [PubMed: 11287133]

McKiernan KA, Kaufman JN, Kucera-Thompson J, Binder JR. A parametric manipulation of factors affecting task-induced deactivation in functional neuroimaging. J Cogn Neurosci 2003;15:394–408. [PubMed: 12729491]

Miller EK, Cohen JD. An integrative theory of prefrontal cortex function. Annu Rev Neurosci 2001;24:167–202. [PubMed: 11283309]

Otten LJ, Rugg MD. When more means less: neural activity related to unsuccessful memory encoding. Curr Biol 2001;11:1528–1530. [PubMed: 11591321]

Pfefferbaum A, Mathalon DH, Sullivan EV, Rawles JM, Zipursky RB, Lim KO. A quantitative magnetic resonance imaging study of changes in brain morphology from infancy to late adulthood. Arch Neurol 1994;51:874–887. [PubMed: 8080387]

Polli FE, Barton JJ, Cain MS, Thakkar KN, Rauch SL, Manoach DS. Rostral and dorsal anterior cingulate cortex make dissociable contributions during antisaccade error commission. Proc Natl Acad Sci U S A 2005;102:15700–15705. [PubMed: 16227444]

Preston AR, Thomason ME, Ochsner KN, Cooper JC, Glover GH. Comparison of spiral-in/out and spiral-out BOLD fMRI at 1.5 and 3 T. Neuroimage 2004;21:291–301. [PubMed: 14741667]

Quigley M, Cordes D, Turski P, Moritz C, Haughton V, Seth R, Meyerand ME. Role of the corpus callosum in functional connectivity. AJNR Am J Neuroradiol 2003;24:208–212. [PubMed: 12591635]

Raichle ME, MacLeod AM, Snyder AZ, Powers WJ, Gusnard DA, Shulman GL. A default mode of brain function. Proc Natl Acad Sci U S A 2001;98:676–682. [PubMed: 11209064]

Reuter-Lorenz P, Jonides J, Smith E, Hartley A, Miller A, Marshuetz C, Koeppe R. Age differences in the frontal lateralization of verbal and spatial working memory revealed by PET. Journal of Cogn Neurosci 2000;12:174–187.

Shulman GL, Fiez JA, Corbetta M, Buckner RL, Miezin FM, Raichle ME, Petersen SE. Common blood flow changes across visual tasks .2. Decreases in cerebral cortex. Journal of Cognitive Neuroscience 1997;9:648–663.

Smith EE, Jonides J, Koeppe RA. Dissociating verbal and spatial working memory using PET. Cereb Cortex 1996;6:11–20. [PubMed: 8670634]

Sowell ER, Thompson PM, Holmes CJ, Jernigan TL, Toga AW. In vivo evidence for post-adolescent brain maturation in frontal and striatal regions. Nat Neurosci 1999;2:859–861. [PubMed: 10491602]

Thomason M, Race E, Burrows B, Whitfield-Gabrieli S, Glover G, Gabrieli J. Development of Spatial and Verbal Working Memory Capacity in the Human Brain. in press

Wagner AD, Shannon BJ, Kahn I, Buckner RL. Parietal lobe contributions to episodic memory retrieval. Trends Cogn Sci 2005;9:445–453. [PubMed: 16054861]

Weissman DH, Roberts KC, Visscher KM, Woldorff MG. The neural bases of momentary lapses in attention. Nat Neurosci 2006;9:971–978. [PubMed: 16767087]

Yakovlev, PI.; Lecours, AR. The myelogenetic cycles of regional maturation of the brain. In: Minkowski, A., editor. Regional Development of the Brain in Early Life. Davis; Philadelphia: 1967. p. 3-70.

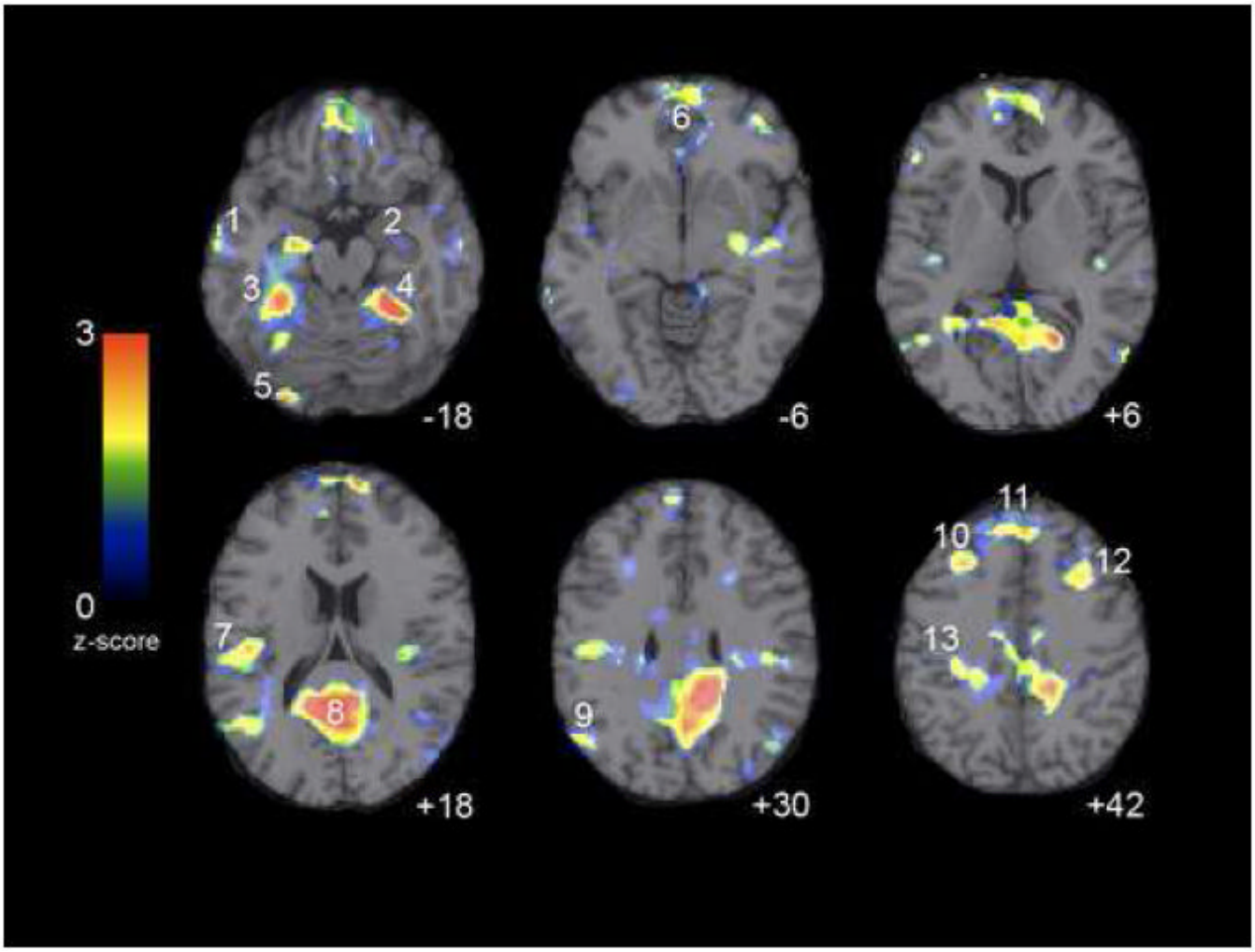

Figure 1.

Areas in which children exhibited load-dependent decreases in activation with increased WM load. Numbers correspond to coordinates listed in Table 2. Peak deactivations were observed in posterior cingulate, precuneus, middle frontal, fusiform, parahippocampal, sensorimotor, and parietal regions. Axial images are presented in neurological convention (left is left) with deactivation threshold set to $p < 0.05$.

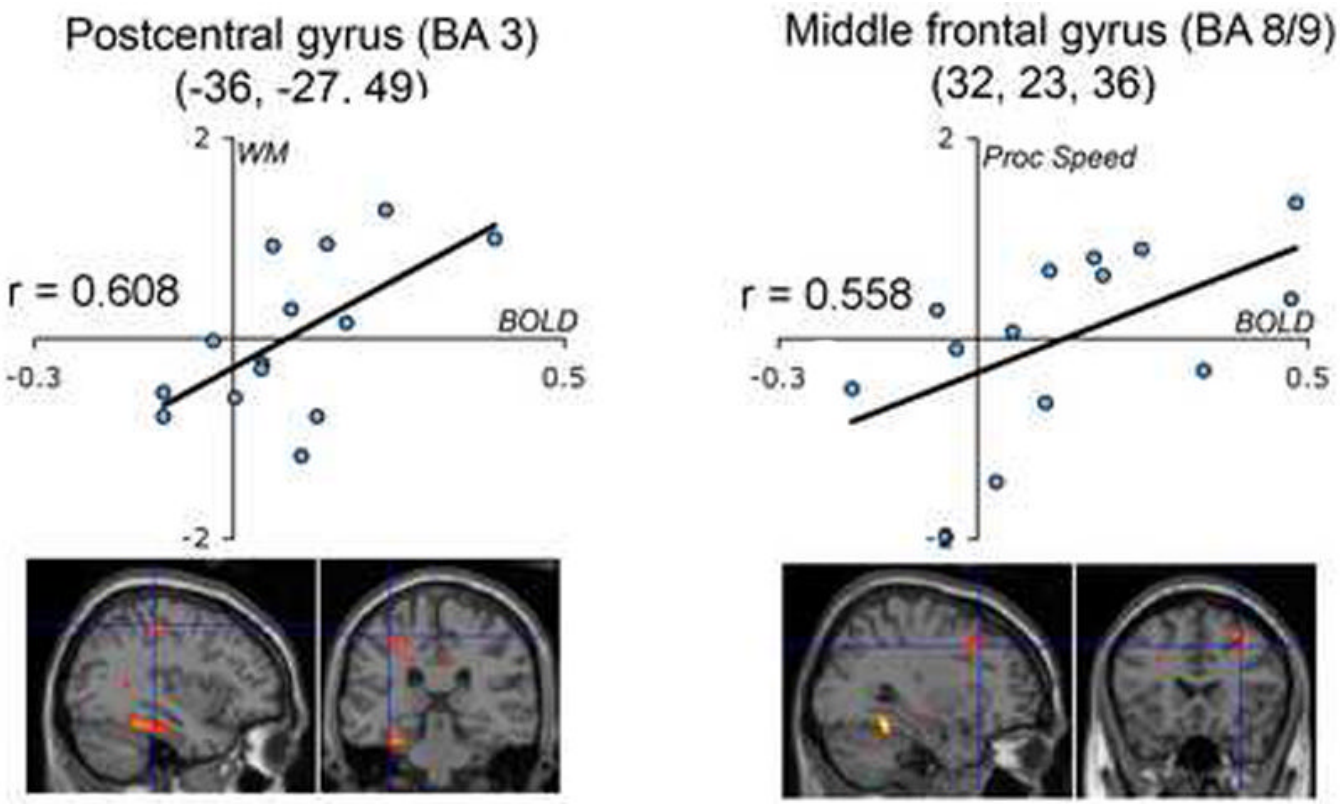

Figure 2.

Cognitive measures administered outside of scanner were significantly correlated with the amount of BOLD decrease between low and high loads at $p < 0.05$ in postcentral and middle frontal gyri. WM = working memory composite z-score across digit and block span; Proc Speed = processing speed composite z-score across digit symbol, visual matching, and cross out.

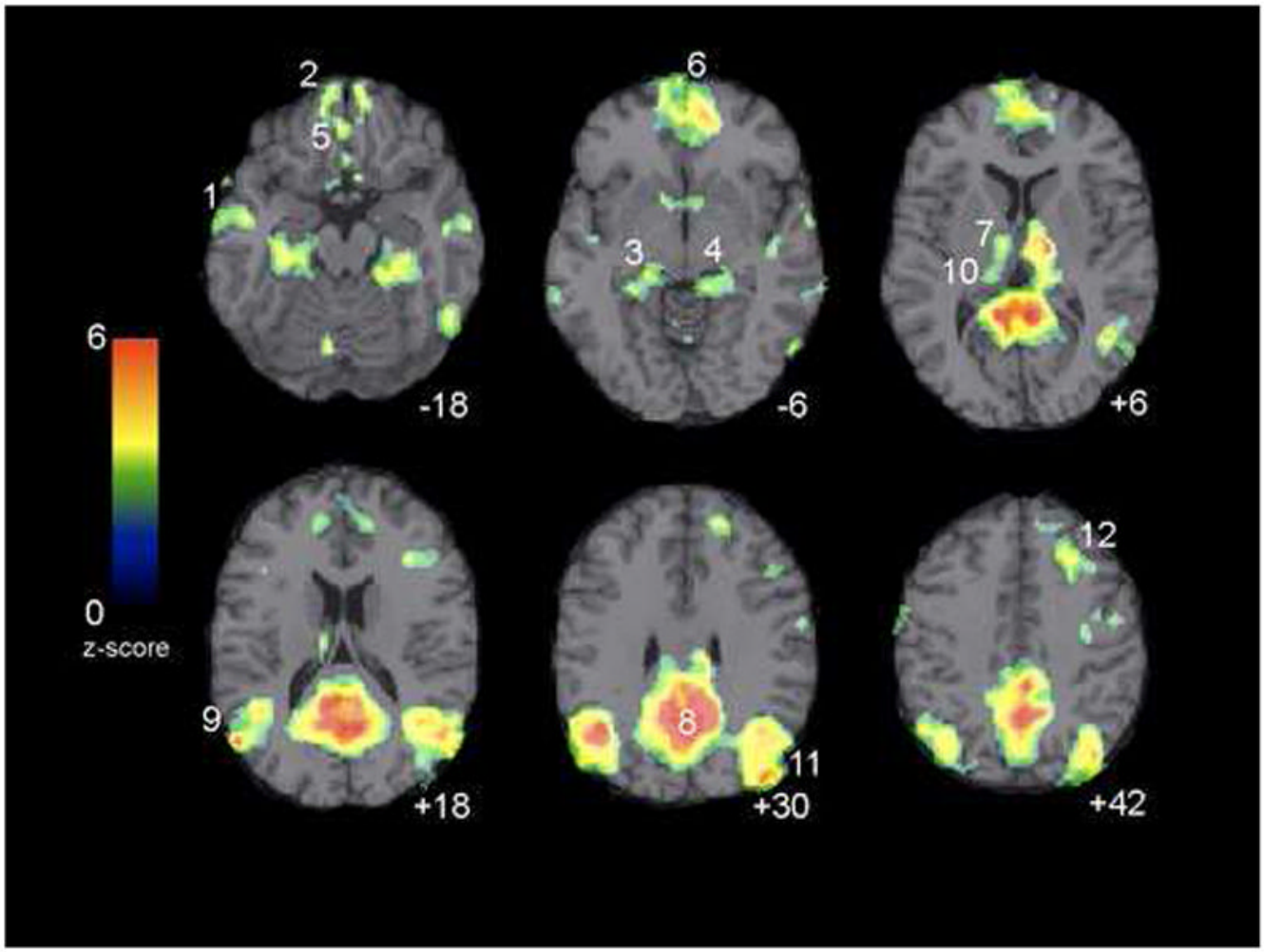

Figure 3.

Areas in which children exhibited default-mode network functional connectivity. z-scores reflect the degree to which a the time series of a given voxel correlates with the time series corresponding to the default-mode network-specific ICA component. Images are thresholded at $p < 0.01$ with cluster minimum of 25 voxels. Numbers correspond to coordinates listed in Table 5. Axial images are presented in neurological convention (left is left).

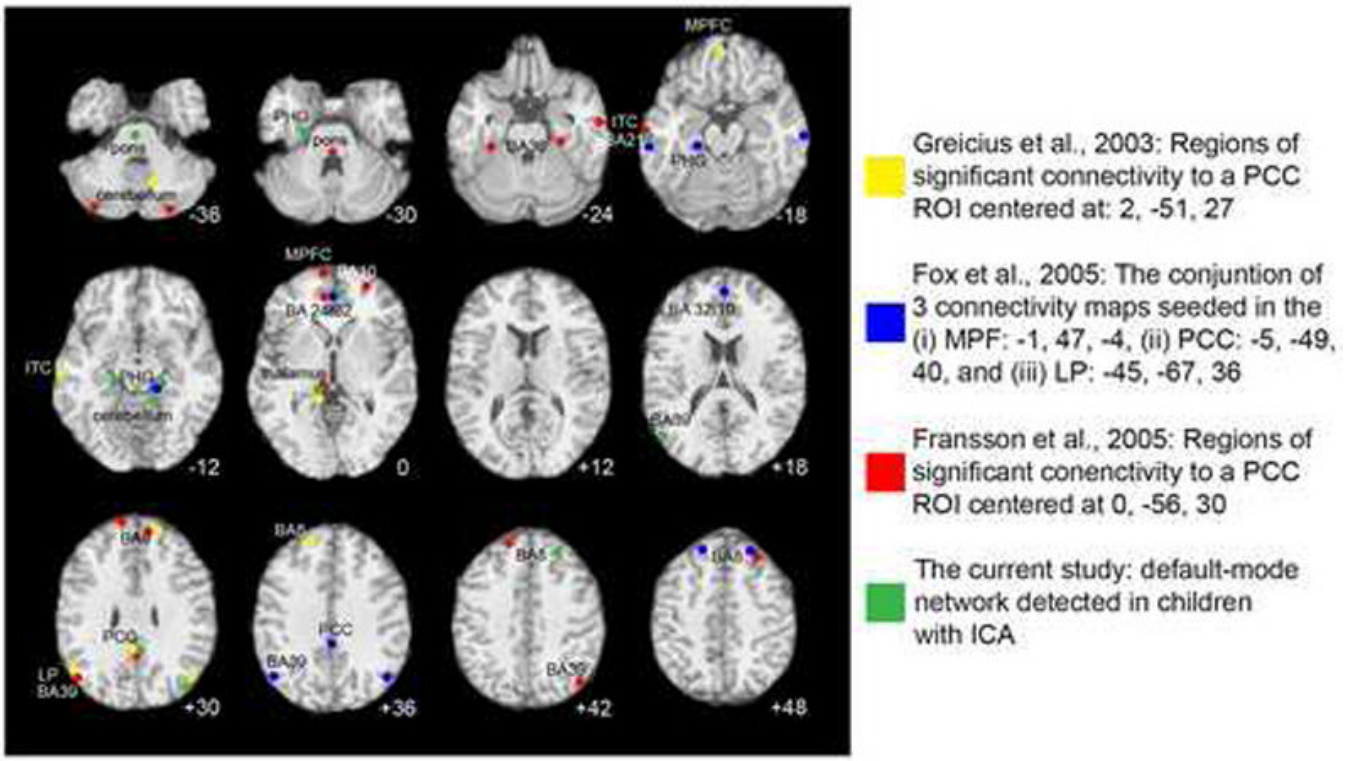

Figure 4.

Peak resting state functional connectivity in the default-mode brain network derived from four studies. Three of the studies used ROI-based functional connectivity analysis in adults, while the current study used ICA-based analysis in children. Abbreviations: PCC, posterior cingulate cortex; ITC, inferolateral temporal cortex; MPFC, medial prefrontal cotex; PHG, parahippocampal gyrus; BA, Brodmann Area. Axial images are presented in neurological convention (left is left). The z coordinate for each peak was adjusted to fall on the nearest representative slice.

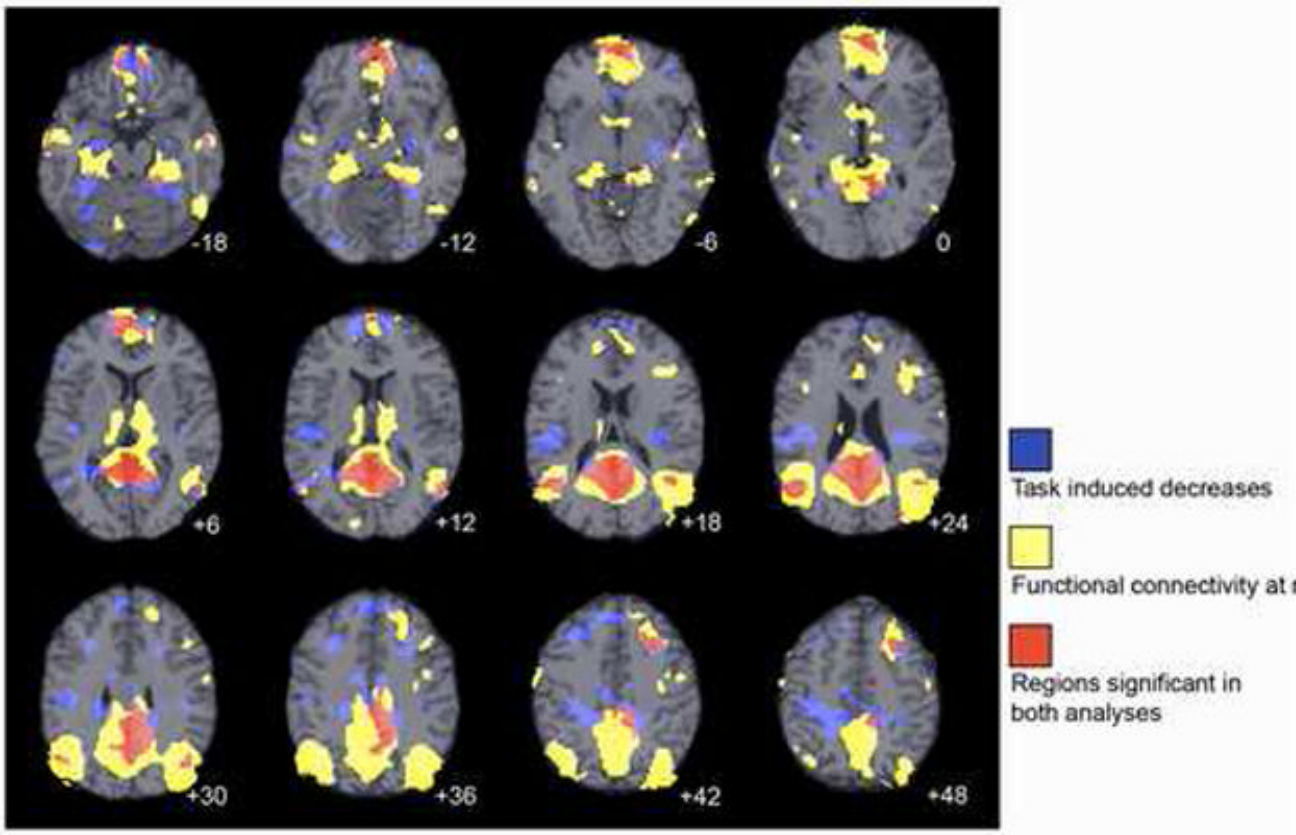

Figure 5.

Regions of task-induced deactivations and ICA-based functional connectivity at rest, and the overlap between them in the default-mode brain network. Axial images are presented in neurological convention (left is left) and z coordinates for each slice are given. Activation maps for WM task-induced deactivations were binarized at a set threshold of $p < 0.05$, and functional connectivity maps were similarly binarized at a set threshold of $p < 0.01$ with a k extent of 25 voxels.

Table 1

Behavioral results

Behavioral results for six working memory (WM) tasks. Within-subject comparisons of spatial versus verbal WM were nonsignificant, indicating that performance was equivalent across spatial and verbal tasks. N = 14.

Load	Measure	Mean (st.dev)	
		Spatial WM	Verbal WM
Lowest	Accuracy	84.72 (10.44)	84.72 (10.66)
Middle	Accuracy	66.47 (17.75)	78.97 (15.04)
Highest	Accuracy	62.5 (11.97)	63.49 (14.15)
Lowest	Median RT	1008 (102)	1037 (117)
Middle	Median RT	1110 (76)	1092 (155)
Highest	Median RT	1156 (138)	1124 (128)

Table 2

Regions of significant task-induced decreases

Regions of significant task-induced decreases for the present study and peak foci for four deactivation studies with adults (Binder et al., 1999; Mazoyer et al., 2001; McKiernan et al., 2003; Shulman et al., 1997) Results from the present study are the product of the conjunction of decreases across both spatial and verbal WM loads. Cluster volumes and peak z-scores are reported for all foci above $p < 0.01$ with a cluster minimum set to 25 voxels. Coordinates are reported in neurological convention in Talairach and Tournoux space. N = 14. D is the calculated Euclidian distance between peaks in previous study and peaks in the present study and is reported in mm. Italicized ROIs were flipped R/L to increase chances of close range in coordinate sampling. Shaded regions were not closely localized to any peaks reported in the adult studies. Δ values (percent signal change) and their associated significance are reported for 10mm spherical ROIs centered on peaks extracted from the adult literature that were tested with the current data.

	Present study						Mazoyer et. al						Binder et. al						McKierman et. al						Shulman et. al. 1997					
	BA	**X**	**Y**	**Z**	**Vol.**	**Z score**	**BA**	**X**	**Y**	**Z**	**D**	**Δ peak**	**BA**	**X**	**Y**	**Z**	**D**	**Δ peak**	**BA**	**X**	**Y**	**Z**	**D**	**Δ peak**	**BA**	**X**	**Y**	**Z**	**D**	**Δ peak**
1	21/20	-59	-1	-20	36	2.13																			20	-49	-19	-18	21	0.056
2	36/35	28	-19	-23	25	2.08																			amygdala	21	-9	-18	13	§0.103
3	20/28/36/34	-30	-38	-15	387	2.36							36	-26	-35	-12	6	*0.075	37	-28	-42	-19	6	***0.154						
4	37*	30	-45	-11	224	2.75							*36*	*26*	*-35*	*-12*	*11*	**0.077*	*37*	*28*	*-42*	*-19*	*8.8*	*0.106						
5	18*	-24	-88	-9	31	1.65																								
6	10*/11/9	-6	66	-7	251	2.25	10	-4	58	12	20.7	*0.187							32	-6	44	1	23.4	0.054	10	-1	47	-4	20	0.14
7	13*/41/43	-46	-19	16	64	1.78																								
8	23*/31/30	-2	-51	25	1202	2.49	31	-6	-50	26	4.2	**0.252	23/31	-9	-55	24	8	**0.154	31	-7	-50	30	7.1	*0.169	31/7	-5	-49	40	15	§0.091
9	39*/22	-48	-63	29	36	1.65	39	-52	-74	18	16.1	0.013	39	-43	-70	26	9	0.028	39	-47	-72	21	12	0.011	39/19	-45	-67	36	9	0.053
10	8*/9	-30	27	39	41	1.75	8	-32	22	42	6.2	0.024	8/9/10	-20	30	44	12	0.042	8	-23	25	46	10	0.015	8	-27	27	40	3	§0.086
11	8*/6/9	4	45	38	31	1.89													8/9	-12	43	41	16.4	0.099	8/9	5	49	36	5	§0.159
12	8*/9	32	23	36	79	1.67	*8*	*32*	*22*	*42*	*6.1*	§*0.108*	*8/9/10*	*20*	*30*	*44*	*16*	*0.04*	*8*	*23*	*25*	*46*	*14*	*0.044*	*8*	*27*	*27*	*40*	*8*	§*0.102*
13	3*/40/4/5/2/7	-36	-27	49	183	1.72																								

§ $p<0.1$,

* $p<0.05$,

** $p<0.01$,

*** $p<0.001$.

Table 3

Regions of deactivations in adults not observed in the present study

Six regions reliably deactivated in studies of adults that did not reach significance in the current study. D = Euclidian distance in mm. Coordinates are reported in neurological convention in Talairach and Tournoux space. Studies included in this summary: Shulman et al., 1997, Binder et al., 1999, Mazoyer et al., 2001, and McKiernan et al., 2003.

Region	Study	BA		X	Y	Z	D
1	mazoyer	2	a	24	-34	64	b/c = 28.4
	mckiernan	7	b	29	-45	57	a/b = 14
	mckiernan	3/4	c	14	-27	73	a/c = 15.2
2	mazoyer	11	a	-26	36	-10	b/c = 18.5
	binder	11	b	-26	28	-8	a/b = 8.2
	shulman	10/47	c	-33	45	-6	a/c = 12.1
3	mazoyer	32	a	0	38	-2	b/c = 12.7
	binder	12/32	b	-9	34	-7	a/b = 11
	shulman	32	c	3	31	-10	a/c = ll
4	mazoyer	46	a	-46	36	18	a/b = 11.9
	binder	45	b	-51	26	14	
5	mazoyer	10	a	-46	48	0	a/b = 14.6
	shulman	10/47	b	-33	45	-6	
6	mazoyer	39	a	46	-68	26	a/b = 13.6
	shulman	40	b	45	-57	34	

Table 4

Behavioral results from tests of processing speed and working memory

Individual participant Z-scores on each test of processing speed and working memory are depicted as rows. Composite values are the combined averages of these scores.

visual matching	cross out	digit symbol	digit span	block span	composite processing speed score	composite working memory score
1.13	0.19	0.68	-1.04	-0.17	0.67	-0.60
-0.23	-0.62	-0.68	1.29	-1.36	-0.51	-0.04
-0.10	-0.89	0.00	-0.46	-1.12	-0.33	-0.79
0.18	-0.35	0.34	1.29	1.26	0.06	1.27
0.45	0.73	0.68	-0.46	1.02	0.62	0.28
1.27	-0.08	1.47	0.12	1.74	0.89	0.93
0.18	0.19	0.45	-0.46	-0.65	0.27	-0.55
1.00	1.81	1.24	0.71	1.26	1.35	0.98
0.31	0.73	0.11	0.12	-0.65	0.39	-0.26
-1.33	-1.43	-1.58	-0.46	-1.12	-1.45	-0.79
-1.19	-0.08	-0.68	0.71	-0.41	-0.65	0.15
-0.37	-0.08	0.11	-0.46	-0.17	-0.11	-0.31
0.86	1.54	0.00	1.29	0.54	0.80	0.92
-2.15	-1.69	-2.15	-2.20	-0.17	-2.00	-1.19

Table 5

Regions of significant functional connectivity across children's default-mode networks

Cluster volumes and peak z-scores are reported for all foci above $p < 0.001$ with a cluster minimum set to 25 voxels. z-scores reflect the degree to which the time series of a given voxel correlates with the time series corresponding to the default-mode network-specific ICA component. Numbering in left column corresponds to labels in Fig. 3. Coordinates are reported in neurological convention in Talairach and Tournoux space. N = 16.

Fig. 3	Region	BA	X	Y	Z	Vol.	Z score
	Medulla and pons	Brainstem	-2	-21	-38	175	4.53
	Uncus and parahippocampal gyrus	28/35/36	-20	-9	-30	86	3.5
1	Inferior and middle temporal	20/21	-61	-16	-18	127	3.48
2	Superior, orbital, rectal, and medial frontal	11	-6	57	-21	74	3.99
3	Parahippocampal gyrus and hippocampus	28/35	-18	-30	-10	200	3.65
4	Parahippocampal gyrus	35/36	22	-35	-10	130	3.53
5	Medial, orbital frontal, and gyrus rectus	11	-2	40	-17	31	3.45
6	Superior & middle frontal, and anterior cingulate	10/32	10	46	-4	875	4.4
7	Ventral lateral & anterior, and medial dorsal nuclei	Thalamus	-8	-11	10	29	3.73
8	Cingulate, precuneus	7/23/31	10	-47	30	6635	5.37
9	Superior & middle temporal, inferior parietal, angular, and supramarginal gyri	39	-53	-65	20	1404	4.64
10	Medial & lateral dorsal, and pulvinar nuclei	Thalamus	-10	-23	12	41	3.72
11	Inferior parietal, precuneus, middle temporal, and angular gyri	19/22/39	44	-80	33	1874	4.67
12	Middle, medial, and superior frontal gyri	8	26	25	41	120	3.49
	Precuneus	7	4	-55	62	58	3.49